Proceedings European Geothermal Congress 2007
Unterhaching, Germany, 30 May-1 June 2007

Tracer-assisted evaluation of hydraulic stimulation experiments for geothermal reservoir candidates in deep crystalline and sedimentary formations

Iulia Ghergut[1], Martin Sauter[1], Horst Behrens[1], Peter Rose[2], Tobias Licha[1], Manuela Lodemann[1] and Steffen Fischer[1]

[1]Univ. Göttingen, GeoZentrum, Goldschmidtstr. 3, 37077 Göttingen, Germany; [2]EGI Utah, USA

iulia.ghergut@geo.uni-goettingen.de, igh@gmx.org

Keywords: EGS, tracer tests, single-well, push-pull, Deep Continental Drilling (KTB), N-German sedimentary basin

ABSTRACT

Tracer tests provide information on transport properties essential for heat exchange in geothermal reservoirs, namely: fluid residence times, fluid-rock contact surface areas – which are not properly captured by hydraulic or geophysical methods. Mostly, tracer tests can be conducted in parallel with hydraulic or hydro-mechanical experiments, without major additional effort. Here, the use of push-pull and flow-path tracing tests to evaluate the effect of hydraulic stimulation measures is illustrated with different field settings, for short- and long-term experiments in deep crystalline and sedimentary reservoirs in Germany.

From the tracer breakthrough curves in the push-pull tests (at the KTB site), the specific (i.e., per-volume) area of the fluid-rock contact surface could be estimated, and its change was used to appreciate the effects of massive stimulation. From tracer BTCs in the hydrofrac spiking test (at the Horstberg site), a fluid residence time distribution was obtained, from which the reservoir's flow–storage characteristics could be derived, and extrapolated tracer recoveries provided an estimate of the flow capture angle to the target horizon.

1. INTRODUCTION

Fluid residence times and transport-effective fracture densities (or specific heat-exchange areas) are two important parameters of subsurface flow systems in fractured-porous formations (or geothermal reservoirs). To determine them, tracer[*] tests are indispensable. Hydraulic and geophysical investigation methods provide no, or only limited access to these two parameters, because the signals on which hydraulic or geophysical test methods rely do not depend on, or do not correlate unambiguously with fluid motion and with solute or heat fluxes across fracture surfaces. Fluid temperature variations accompanying hydraulic operations do, in principle, reflect these parameters, but usually high thermal diffusivities make temperature signals rapidly reach quasi-equilibrium values, obliterating parameter dependencies (especially those that would become critical in the long run).

Before reporting on a series of tracer applications for characterizing candidate geothermal reservoirs in deep crystalline and sedimentary formations in Germany, a brief account is given of how artificial tracing methods can be used to determine the two above-named parameters, and how the sensitivity of their determination depends on the kind of method used (cf. fig. 1): inter-well or intra-well flow-path tracings (FP), or single-well tracer injection-withdrawal (SWIW; with the tacit understanding that in FP spiking and sampling take place at different locations A and B within a flow field in which there is a non-zero fluid discharge component from A to B, whereas in SWIW injection/spiking and withdrawal/sampling are into and from one and the same screening interval of a borehole). For the purposes of this contribution, we find it appropriate to revisit some of the basic notions of both type of methods. While FP tracings are commonly used, being discussed in almost any textbook on hydro/geological investigation methods, SWIW tracing applications are less popular, and in the literature to date they seem to be reserved for rather exotic investigation purposes (Novakowski et al. 1998, Haggerty et al. 2001). They could, however, start receiving more attention within the various deep-geothermics projects, since the usual setting to start with in a deep-geothermal project is that just one borehole is available, and if it screens just one target formation then only SWIW tracings can be conducted there.

[*] throughout this paper, the word 'tracer' refers to artificial tracers only, that are purportedly introduced into a system at a given, narrowly-localized time and place; environmental tracers, whether natural or man-made, are not addressed.

2. BASIC NOTIONS, REVISITED

Fluid residence times are usually quantified in terms of a mean residence time (MRT) together with a residence time distribution (RTD), which may in turn be specified by one or more parameters. The MRT in the mobile-fluid compartment of a system, or, empirically, how long it takes for a transport-REV-size fluid particle to travel from A to B, is equivalent to the size of the reservoir accessed between A and B, irrespective of whether A and B represent two boreholes, or two screening intervals at one and the same borehole (cf. fig. 1). To determine it, a flow-path tracing is required, i. e. by spiking the fluid entering the system at A and sampling the spiked fluid at B. In general, the RTD of a tracer need not be identical with the RTD of the fluid in the mobile-fluid compartment; even for an ideal tracer, its RTD depends on the boundary conditions associated with injection and sampling, thus systematically differing from the fluid RTD. However, the natural way tracer injection and tracer sampling are performed in practice does correspond to the so-called 'flux' mode (cf. Zuber 1986), which for an ideal tracer ensures that its breakthrough curve (BTC) measured at B, normalized by the tracer quantity injected at A, directly provides the required fluid residence time distribution in the system accessed between A and B. In principle, knowledge of the fluid RTD, between any two points of a system, will completely characterize a flow field under the given hydraulic conditions; often, it is interesting to know how the RTD changes when hydraulic conditions change. Generally, for tracer applications, there are basically two situations of interest: in natural or in forced flow fields. If spiking and sampling are conducted at one and the same point in a natural flow field, tracer dilution will only relate to the fluid velocities carrying solute away from this point – the basic idea underlying the point dilution method

(Drost et al. 1968, using radioisotopes) for determining groundwater velocities; Bachmat and Behrens (1980), Novakowski et al. (1998; 2006) refined and developed this concept into a SW method for determining the transport properties of a target fracture. SWIW tests as mentioned earlier mostly use forced gradients and do not aim at determining flow velocities.

To describe, quantify and experimentally determine the fluid-rock contact-surface area (in particular: the fracture density) in a heterogeneous fractured-porous system, no universal parameter and method exists. Any quantitative approach will depend on how the void space (available for fluid flow and storage) is conceptualized. Fig. 1 shows two extreme types of flow and transport medium: 'granular' vs. fractured (not to be identified with un/consolidated). In sedimentary formations, permeable regions can be described only as superpositions of both types. For deep crystalline formations, the 'pure' fractured description may suffice for most purposes, in which case the fracture density is directly equivalent to the specific (i.e., per-bulk-medium-volume) fluid-rock contact-surface area; but, even with this drastic simplification, its 'effective' value may still depend upon the type of process used to determine it.

2.1 Numerical Treatment of Surface-Related Term(s)

For the tracer applications in radial flow mentioned in this paper, solute or heat transport are assumed to be governed by PDE systems of this type:

$$\phi_f R_f \partial_t C + \frac{\pm|Q|}{2\pi r B}\partial_r C - \alpha\frac{|Q|}{2\pi B}\frac{1}{r}\partial_r\left(\partial_r C\right) = \sigma_m \phi'_m D_m \left(\partial_z C_m\right)_{z=0}$$

$$\begin{array}{rl} & \left(\sigma_m R_m \partial_t - \partial_z \sigma_m D_m \partial_z\right) C_m = 0 \\ \text{IC} : & C_m\left(x,z,t=0\right) = 0 \\ \text{BCs} : & C_m\left(x,z=0,t\right) = C_f\left(x,t\right) \\ & \text{and } \partial_z C_m\left(x,z=z_{\max},t\right) = 0 \end{array}$$

with C, C_m, $f_{f,m}$ and $R_{f,m}$ denoting fracture-domain and matrix-domain concentrations or normalized temperature signals $(T_{unpert} - T) / T_{unpert}$, porosities and sorption-related retardation factors for solutes in these void-space regions, respectively (R=1 for heat and non-sorbing solutes), and s_m the fluid-rock specific contact-surface area, related to the effective size of matrix blocks L_m and to f_f by

$$s_m = (1 - f_f) / L_m$$

The PDE for either heat or solutes can be written as (with L the linear advection–dispersion operator, and with $t_D = R_m^{-1} t/(D_m/L_m^2)$ a dimensionless time variable):

$$\begin{array}{rcl} LC & = & g\left(t_D\right) * \partial_t C \\ & & \text{with } L \equiv R_f\phi_f\partial_t + v_f\partial_x - \partial_x\phi_f D_f\partial_x \\ & & \text{and } g\left(t_D\right) \equiv -\sum_{n=1}^{\infty} a_n \exp\left(-\alpha_n^2 \cdot t_D\right) \end{array}$$

The convolution kernel g is found to admit following truncation:

$$g_{N_{\text{trunc}}}\left(t_D\right) = \begin{cases} -\frac{1}{\pi\sqrt{t_D}} & \text{for } t_D < t_D^*\left(N_{\text{trunc}}\right) \\ -\sum_{n=1}^{N_{\text{trunc}}} a_n \exp\left(-\alpha_n^2 \cdot t_D\right) & \text{for } t_D > t_D^*\left(N_{\text{trunc}}\right) \end{cases}$$

that is more conveniently written as (cf., for instance, Carrera et al. 1998)

$$\begin{array}{rcl} g_{N_{\text{trunc}}}\left(t_D\right) & = & -\left(1 - \sum_{n=1}^{N_{\text{trunc}}} \frac{a_n}{\alpha_n^2}\right)\delta\left(t_D\right) \\ & & - \sum_{n=1}^{N_{\text{trunc}}} a_n \exp\left(-\alpha_n^2 \cdot t_D\right) \end{array}$$

in which the coefficient multiplying the Dirac function can be calculated as

$$\begin{array}{l} 1 - \sum_{n=1}^{N_{\text{trunc}}} \frac{a_n}{\alpha_n^2} = \frac{2}{\pi^2}\Gamma\left(1; \frac{1}{2} + N_{\text{trunc}}\right) \\ = 0.189,\ 0.099,\ 0.040,\ 0.020,\ 0.010,\ 0.004, \ldots \\ \text{for } N_{\text{trunc}} = 1,\ 2,\ 5,\ 10,\ 20,\ 50, \ldots \end{array} .$$

Thus the original PDE system can be transformed into one PDE for C_f, coupled with a finite number of ODEs for the source terms J_n, with truncation-order dependent coefficients – the rougher the truncation, the stronger the apparent retardation associated with matrix diffusion; one has:

$$A_0 \to 1 \text{ and } A \to 0 \text{ when } N_{\text{trunc}} \to \infty$$

and the system to solve reads:

$$\underbrace{\left(R_f\phi_f + \frac{A}{2}R_m\phi_m\right)}_{\substack{\text{partial retardation factor} \\ \text{(diffusion-independent)}}} \partial_t C_f\left(x,t\right) \underbrace{+ v_f\partial_x C_f\left(x,t\right) - \phi_f D_f \partial_{xx} C_f\left(x,t\right)}_{\text{advection-dispersion}} =$$

$$\underbrace{-A_0\frac{R_m\phi_m}{T_m}C_f\left(x,t\right)}_{\substack{\text{diffusion-limited sorption into the matrix} \\ \text{(to include with effective retardation)}}} + \underbrace{R_m\phi_m\frac{h\left(t\right)}{T_m}C_f\left(x,0\right)}_{\text{initial condition 'propagator'}}$$

$$+ \frac{R_m\phi_m}{T_m^2}\sum_{n=1}^{N_{\text{trunc}}} a_n\alpha_n^2 \underbrace{J_n\left(x,t\right)}_{\substack{\text{a number of mutually independent,} \\ \text{time-dependent 'sources',} \\ \text{linearly coupled to } C_f}}$$

$$\frac{\partial}{\partial t}J_n\left(x,t\right) = C_f\left(x,t\right) - \frac{\alpha_n^2}{T_m}J_n\left(x,t\right) \ ,$$

yielding, when the method of lines is used for solution, the following ODE system:

$$\left(R_f\phi_f + \frac{A}{2}R_m\phi_m\right)C'_f\left(t\right) = -A_0\frac{R_m\phi_m}{T_m}C_f\left(t\right) + \frac{R_m\phi_m}{T_m^2}\sum_{n=1}^{N_{\text{trunc}}} a_n\alpha_n^2 J_n\left(t\right)$$

$$J'_n\left(t\right) = C_f\left(t\right) - \frac{\alpha_n^2}{T_m}J_n\left(t\right)\ ,\ J_n\left(0\right) = 0$$

which can be solved numerically at relatively low computational effort (for the examples mentioned here, *Mathematica3.0*'s `NDSolve` was used).

2.2 Parameter Sensitivity Issues

In general, tracer BTCs in FP tracings exhibit much higher sensitivity to advection-related parameters, than tracer BTCs in SWIW tests. However, unlike sometimes stated, even in mainstream sources (e.g., Haggerty et al. 2001), a SWIW procedure, albeit largely insensitive to advection-related parameters and highly sensitive to surface-related parameters, is not able to reduce the sensitivity of BTCs w. r. to hydrodynamic dispersion parameters, and it does not bring any improvement regarding the famous 'empirical indiscernability' between the various processes (hydrodynamic dispersion, matrix diffusion, sorption, multiple-compartment flow and exchange, 'heterogeneity' in general) whose added contributions are responsible for BTC tailings.

One major difference between solute and heat transport resides in the value of Dm, which in low-porosity crystalline rock is several orders of magnitudes higher for heat than for solutes. As a consequence, heat will be able to ‘see’ a larger scale in space and will yield more ‘rapid’ signals in time.

2.3 Time-Moment Analysis of Tracer (Fluid) RTDs

A useful representation of flow-storage characteristics (fig. 2) is provided by a cumulative, truncated-temporal moments diagram: a parametric plot of the 0^{th}-order, time-*t*-truncated moment, against the 1^{st}-order, time-*t*-truncated moment of tracer concentrations, with time *t* as a parameter, shows what fraction of reservoir flow takes place in any fraction of reservoir storage (cumulatively). Similar approaches have been used by Behrens (oral communication, 1998) and Shook (2003).

3. USING TRACER METHODS TO CHARACTERIZE DEEP, CANDIDATE GEOTHERMAL RESERVOIRS IN GERMANY

For candidate geothermal reservoirs in deep formations in Germany, fluid spiking experiences are not very numerous. A systematic campaign of deep-crustal fluid spiking applications was made possible since 2003 with a basic research project funded by the German Research Foundation (DFG) within its Priority Program engagement to the ICDP. This tracer test campaign comprised SW push-pull tracings, as well as a SW and a inter-well FP tracing, in crystalline (KTB, Urach) and sedimentary (Horstberg) formations in ~4 km depth (cf. fig. 1). The tracer tests’ main endeavor was to help understanding processes associated with fluid transport in the deep crust, while also assisting in the quantitative evaluation of hydraulic stimulation measures – which were either short-term, high-rate (Urach, Horstberg) or long-term, moderate-rate (KTB). Further it was hoped that, via the integral parameters they usually provide, tracer tests would reduce the dependency of characterization and prognosis tools upon the availability of detailed discretizing site models and powerful numerical solvers. A subsidiary aim of these tracer tests was to probe the behavior of a number of organic tracers, a priori believed as ‘good’, under the physicochemical conditions of target formations (>100°C, saturated brine, very low redox potential, broad pH range etc.).

3.1 FP Tracing in 4 Km Deep Sandstone/Claystone Formation in N-German Sedimentary Basin

At the Horstberg site in the Northern-German sedimentary basin, a former gas exploration borehole is available for geothermal research and for testing various heat extraction schemes (Jung et al., 2005) in supra-saline horizons. After several geophysical and hydraulic (stimulation) tests (2003 – 2004) not accompanied by fluid spikings, a combined hydro-mechanical and tracer test sequence (fig. 2) was started in late 2004. Using the hydro-frac technique, a large-area fault was created in the heterogeneous formation at ~3.8 km depth, comprising two sandstone layers separated by less permeable, clayey sandstone layers (with a total thickness of ~120 m). Assuming that the induced fault will maintain sufficient permeability over time (without the need for proppants), and that the same result can be achieved at many other similar formations in the Northern-German sedimentary basin, a low-cost single-well, two-layer circulation scheme (described by Jung et al. 2005) is endeavored for heat extraction by the Leibniz Institute for Applied Geosciences (GGA) and the Federal Institute of Geosciences and Natural Resources (BGR) in Hannover.

In order to better characterize the flow in the induced fault, a SW FP tracing was conducted in early post-stimulation state by spiking the fluid injected at the lower horizon and sampling the fluid produced from the upper horizon, with expectably high tracer dilution due to the divergent flow field (fig. 2). After a 1.5-year shut-in phase, short outflow phases from both the production and the former injection horizon yielded further information, of both FP and SWIW type; tracer analytics for these late BTCs is under completion. Extrapolated tracer recoveries from the early test phase showed that up to 12 % of the (more or less radially divergent) flow field is focused to the production screen. Further, a useful characterization of the induced hydrofrac properties is provided by the flow-capacity diagram derived from tracer BTCs (fig. 2), indicating what percentage of the fault flow takes place in any percentage of the fault’s storage.

3.2 Further Tracer Applications in the N-German Sedimentary Basin, as of Mid 2007 (Gr.Schönebeck)

At the *In-situ Geothermal Laboratory* managed by the GFZ Potsdam in GroßSchönebeck in the NE German sedimentary basin (Huenges et al. 2006), two newer boreholes, deemed as GS3 and GS4 (of which the latter is currently under completion), reaching down to sub-saline horizons, are envisaged for further tests. Comprehensive geophysical investigations and hydraulic/mechanical tests have already been conducted at GS3 and neighboring holes in the same or similar formations (Zimmermann et al. 2005). At the new hole GS4, the GFZ Potsdam plans to conduct, as of 2007, a sequence of short-term, high-rate faultings in ~4 km deep volcanics and sandstones, followed by short- and mid-term flow-back tests, and by a long-term, moderate-rate produc¬tion test, with fluids produced at GS4 to be reinjected at GS3.

The first task was to design and dimension several spikings at both boreholes, such that each individual spiking potentially yields measurable signals during each of the subsequent outflow or abstraction phases.

There are to be 4 spikings accompanying the faulting, injectivity and sequential flow-back tests at GS4, whereas the re-injected fluids, at GS3, shall be spiked just once, at the beginning of re-injection (fig. 3, upper part). Forward simulations and sensitivity analyses (fig. 3) were undertaken as an aid in dimensioning the tracer slugs and sampling phases, based on a simplified, radial flow and transport model of the induced or stimulated fractures. From these analyses, tracer signals from flow-back (push-pull) tests at GS4 appear to be more sensitive to effective aperture and specific contact-surface area (within the volume accessed by each test phase), than to the total reservoir size, whilst tracer signals at GS4 but originating from re-injection at GS3 appear to be very sensitive to the total reservoir size, and also to dispersion and surface/exchange parameters (fluid-rock contact-surface area, im/mobile exchange rates or alike).

3.3 Single-well tracer push-pull test in deep crystalline formation at the Urach site

At the 4-km deep borehole Urach-3 in the SW German crystalline (pilot geothermal plant), only one short-term SWIW test was conducted (2003), comprising: three-week, high-rate fluid injection for permeability enhancement of possibly several fracture systems in 2.8 – 4 km depth;

followed by tracer SWIW test (~2 weeks), shut-in (~3 weeks), new outflow phase (~1 week); produced spiked fluids had to be disposed of into the same borehole, which somewhat impairs on future tests using analytically similar tracers in the same reservoir. Tracer SWIW signals did reflect the presence of several fractures in different depths, but their unambiguous quantification seems difficult to achieve in terms of this sole tracer test. A major drawback with the test at the Urach site was that the tracer mass actually entering the target system cannot be estimated reliably (due to a problem during tracer injection); without proper normalization, tracer BTCs cannot be interpreted correctly.

Thus, the tracer tests conducted at the KTB pilot hole in depleted, stimulated and post-stimulation reservoir state – as described in more detail in the next section – remain, for the time being, the only SWIW tracing applications in a deep crystalline formation in Germany for which a consistent interpretation was possible.

3.4 Tracer Tests at Pilot KTB Hole in Depleted, Stimulated and Post-Stimulation Reservoir State

At the German site of ICDP, called *Kontinentale Tiefbohrung* (KTB), two boreholes are available in the crystalline basement: the 4-km deep pilot hole, and the 9-km deep main hole. Owing to extra-ordinary research opportunities enabled by a DFG research project during 2003 – 2006, a combination of short- and long-term tracings could be applied in parallel with a long-term hydraulic, geophysical and seismic testing program, the latter being described in more detail by Kümpel et al. (2006). The pilot KTB hole is known to intersect a relatively permeable fracture system in 3.8 – 4 km depth (Kessels et al. 2006), and is fully cased except for this interval. Here, solute and heat push-pull tests, all of the SWIW type discussed in the preceding contribution, were performed in the depleted (2004), the stimulated (2005a), and the early post-stimulation (2005b) state, with a late outflow phase (2006) in the still weakly pressurized, late post-stimulation state (fig. 4).

Tracer breakthrough curves (BTCs) from solute push-pull tests (fig. 5), and temperature responses from heat push-pull tests (fig. 6), respectively, enable to estimate two parameters:

– a transport-effective contact-surface area per volume between fractures and rock matrix (or a transport-effective fracture density) deemed as *S*, and

– an effective radial extension *R* of the accessed reservoir (or the space scale 'seen' by the tracers),

while other flow– and transport–related parameters are assumed as known, or the tracer BTCs exhibit such poor sensitivity w. r. to these parameters that their values do not matter for the estimation of *S* and *R*. In general, this estimation will slightly depend upon the type of conceptualization used for the fracture network, and upon the kind of exchange processes or fluxes assumed across or close to fracture surfaces.

The effects of long-term depletion (by fluid abstraction, 2003-2004) and of long-term stimulation (by fluid injection, 2004-2005) on the fracture network around the pilot KTB hole were sensitively reflected by solute and heat push-pull BTCs in terms of *S* and *R*, with good sensitivity especially w. r. to parameter *S*. The solute tracer test in the depleted system indicates higher values of *S* and *R* (for an equal chaser volume), than in the stimulated system; the post-stimulation, still weakly pressurized state of the system is characterized by intermediate values of *S* and *R*; whereas the heat push-pull tests which paralleled the solute push-pull tests yield complimentary far-field values:

$$S_{\text{stimulated, far-field}} > S_{\text{stimulated, near-field}}$$

$$S_{\text{depleted, far-field}} < S_{\text{depleted, near-field}}$$

$$R_{\text{stimulated}} < R_{\text{depleted}} \ , \quad R_{\text{solute tracers}} < R_{\text{heat}}$$

This implies (cf. fig. 7) that the prevailing effect of long-term, moderate-rate, cold-fluid injection was to enlarge pre-existing fractures, rather than creating new ones – despite some expectations that cooling-induced cracking would prevail; or, even though (micro-)cracking might have occurred extensively, these (micro-)cracks' contribution to heat and solute transport was overwhelmed by the contribution of preexisting fractures.

The heat push-pull test in post-stimulation state (2005, ~4 months after the end of fluid injection and the last spiking, and ~6 months after the previous spiking, cf. fig. 4) provided the opportunity of an interesting extension to the solute tracer information. Given the short-term nature of this test, concentration changes during withdrawal phases are approximately linear; given the different weightings of the two tracers' quantities between the successive slugs, one tracer is increasing while the other is decreasing in concentration (fig. 8); a quantitative interpretation of these particular signals was not attempted as yet.

Finally, it is worth mentioning that the first spiking under stimulation conditions (second tracer slug on fig. 4) might produce detectable signals during a future production test at the main hole; it will, however, experience very high dilution due to:

– divergent flow field during chaser injection at the pilot hole

– large contribution of unspiked fluid during fluid production at the main hole (cf. fig. 10),

with a number of transport (and thermal decay) scenarios being illustrated in fig. 9. Existence, location and geometry of a fracture system connecting the two boreholes are not known beforehand.

4. SUMMARY OF EXPERIENCES GAINED

From tracer BTCs in SWIW tests (at the KTB site), the specific area of the fluid-rock contact surface could be estimated, and its change with different hydraulic regimes was used to appreciate the effect of hydraulic stimulation (cf. fig. 7). From tracer BTCs in the hydrofrac push test (at the Horstberg site), the fluid RTD was derived and analyzed, thus the flow–storage properties of the accessed reservoir could be characterized (cf. fig. 2), and the flow capture angle to the target horizon could be estimated from the tracer recovery. In all cases described, tracer tests are conducted in parallel with hydraulic tests or stimulation measures, without significant additional expenses.

Regarding organic tracer behavior, it is worth mentioning that uranine (di-Na-fluorescein), used as a tracer in all tests, showed systematically lower recoveries than the other, simultaneously injected organic tracers (cf. figs. 1, 3); a massive conversion to its leuco-dye form (reduction reaction in-situ), during the hydro-frac tracing in the

Horstberg sedimentary formation, was identified, explained and quantified by Behrens et al. (2006).

5. OPEN ISSUES, NEED FOR FURTHER RESEARCH

Good knowledge of the tracers' physicochemical behaviour under given reservoir conditions, sensitive and reliable tracer analytics (Behrens 1971; 1986) are prerequisite for the correct interpretation of test results. Major differences between BTCs of several simultaneously injected organic tracers, as seen in the KTB and Horstberg tests (Behrens et al. 2006), far beyond what one would expect from their different molecular diffusion, graphically demonstrate the need for more research on these issues. During the forthcoming stimulation at GroßSchönebeck in the N-German sedimentary basin, SW fluid spikings at 4 different stages and one inter-well FP tracing are planned, all tests more or less overlapping with each other. For a correct interpretation of these tests, at least 3 conservative solute tracers should be available; moreover, their analytics should meet reasonable detection limits in saturated brine, for the necessary tracer quantities to inject not to become prohibitive.

Acknowledgements to the German Research Foundation (DFG) and to the German Ministry for Environment (BMU) for long-term financial support (DFG grants Sa 501 / 16 / 1–4 and Sa 501 / 21 / 5, BMU project no. 0327579). Thanks to R. Jung, H.-J. Kümpel, J. Orzol, R. Jatho, T. Tischner, K. Hofmeister, R. Junker, H. Evers and colleagues from the Leibniz Institute for Applied Geosciences (GGA) and the Federal Institute for Geosciences and Natural Resources (BGR) Hannover, to G. Zimmermann and E. Huenges from the Geoscientific Research Centre (GFZ) Potsdam for personnel and financial assistance during the execution or preparation of field tests, and for valuable scientific cooperation.

REFERENCES

Bachmat, Y., and Behrens, H.: Entwicklung von Einbohrlochtechniken zur quantitativen Grundwassererkundung. *GSF-Berichte, R* **369** (1984), München.

Behrens, H.: Untersuchungen zum quantitativen Nachweis von Fluoreszenzfarbstoffen bei ihrer Anwendung als hydrologische Markierungsstoffe. *Geologica Bavarica*, **64** (1971), 120-131.

Behrens, H.: Water Tracer Chemistry – a Factor Determining Performance and Analytics of Tracers. *Proceedings*, 5th Symposium on Underground Water Tracing, Athens (1986), 121-133.

Behrens, H., Ghergut, I., Licha, T., Orzol, J., and Sauter, M.: Reactive behaviour of uranine (fluorescein) in a deep geothermal-reservoir tracer test. *Geophysical Research Abstracts*, **8** (2006), 10448.

Carrera, J., Sanchez-Vila, X., Benet, I., Medina, A., Galarza, G., and Guimera, J.: On matrix diffusion: formulations, solution methods and qualitative effects. *Hydrogeology Journal*, **6** (1998), 178-190.

Drost, W., Klotz, D., Koch, A., Moser, H., Neumaier, F., and Rauert, W.: Point dilution methods of investigating ground water flow by means of radioisotopes. *Water Resources Research*, **4** (1968), 125-146.

Erzinger, J., and Stober, I.: Introduction to Special Issue: long-term fluid production in the KTB pilot hole, Germany. *Geofluids*, **5** (2005), 1–7.

Gräsle, W., Kessels, W., Kümpel, H.-J. and Li, X.: Hydraulic observations from a one year fluid production test in the 4000 m deep KTB pilot borehole. *Geofluids*, **6** (2006), 8–23.

Haggerty, R., Fleming, S.W., Meigs, L.C., and McKenna, S.A.: Tracer tests in a fractured dolomite, 2, Analysis of mass transfer in single-well injection-withdrawal tests. *Water Resources Research*, **37** (2001), 1129-1142.

Huenges, E., Trautwein, U., Legarth, B., and Zimmermann, G.: Fluid pressure variation in a sedimentary geothermal reservoir in the North German Basin: Case study Groß Schönebeck. *Pure and Applied Geophysics*, **163(10)** (2006), 1-12.

Jung, R., Orzol, J., Jatho, R., Kehrer, P., and Tischner, T.: The GenESys Project: Extraction of Geothermal Heat From Tight Sediments. *Proceedings*, 30th Workshop on Geothermal Reservoir Engineering, Stanford University, Stanford, CA, *SGP-TR*-**176** (2005).

Kessels, W., Kaiser, R., and Gräsle, W.: Hydraulic Test Interpretation with Pressure Dependent Permeability – Results from the Continental Deep Crystalline Drilling in Germany. *Proceedings*, 2nd International Symposium on Dynamics of Fluids in Fractured Rock, Berkeley, CA (2004).

Kümpel, H.-J., Erzinger, J., and Shapiro, S.A.: Two Massive Hydraulic Tests Completed in Deep KTB Pilot Hole. *Scientific Drilling*, **3** (2006), 40–42.

Novakowski, K.S., Lapcevic, P.A., Voralek, J.W., and Sudicky, E.A.: A note on a method for measuring the transport properties of a formation using a single well. *Water Resources Research*, **34(5)** (1998), 1351–1356.

Novakowski, K., Bickerton, G., Lapcevic, P., Voralek, J., and Ross, N.: Measurements of groundwater velocity in discrete rock fractures. *Journal of Contaminant Hydrology*, **82** (2006), 44–60.

Shook, G.M.: A Simple, Fast Method of Estimating Fractured Reservoir Geometry from Tracer Tests. *Geothermal Resources Council Transactions*, **27** (2003), 407-411.

Zimmermann, G., Burkhardt, H., and Engelhard, L.: Scale dependence of hydraulic and structural parameters in fractured rock, from borehole data (KTB and HSDP). In: Harvey, Brewer, Pezard, and Petrov (Eds.), *Petrophysical properties of crystalline rocks*, Geological Society of London (2005), 37-45.

Zuber, A.: Review of existing mathematical models for interpretation of tracer data in hydrology. Intl. Atomic Energy Agency, Vienna, *IAEA–TECDOC* **381** (1986), 69-116.

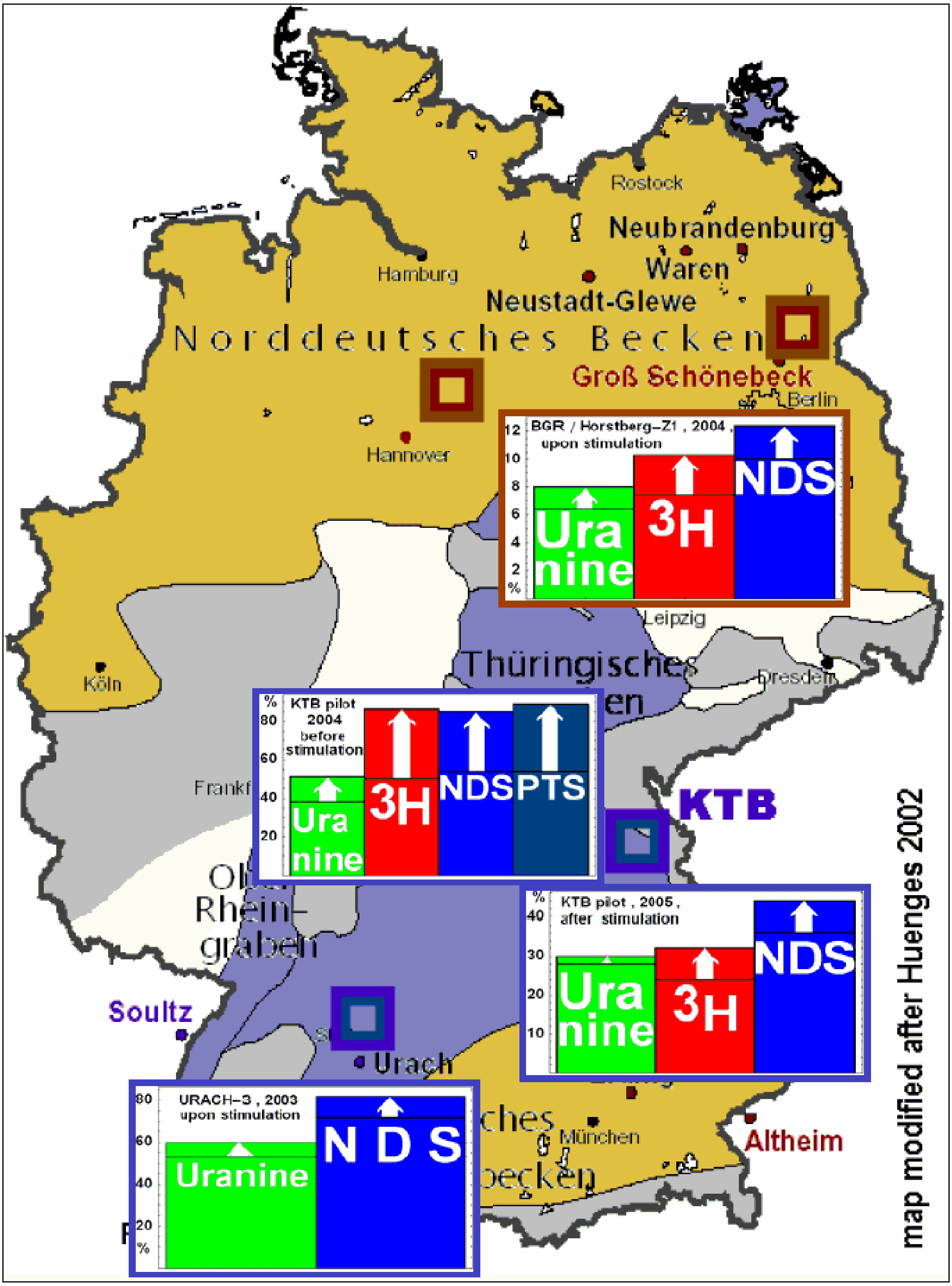

Figure 1a: Test sites (framed in blue: deep crystalline, in brown: N-German sedimentary basin); tracers used and their (actual, versus extrapolated) recoveries; recovery extrapolation, where applicable, is by integrating until free outflow rates would approach zero.

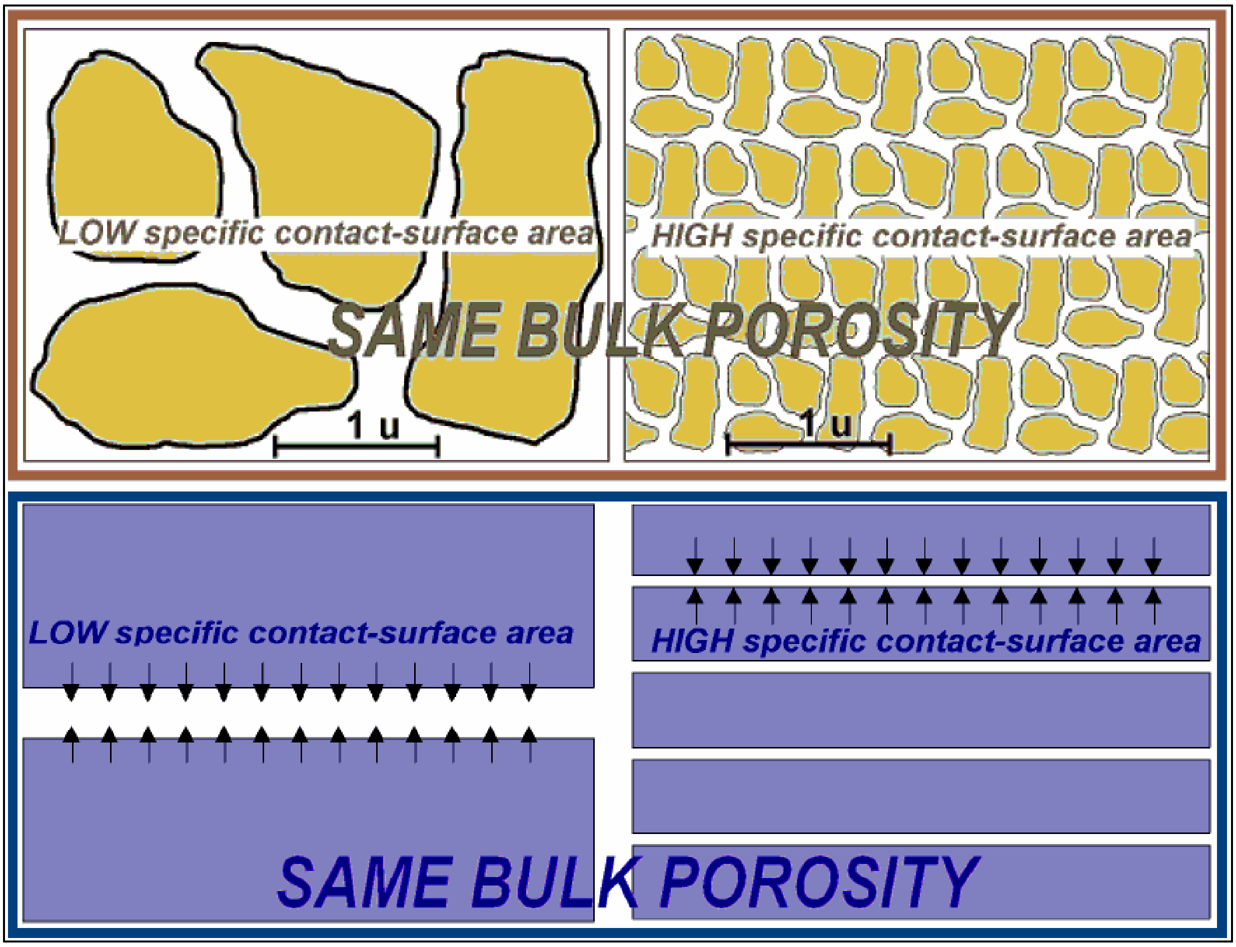

Figure 1b: Formation types.

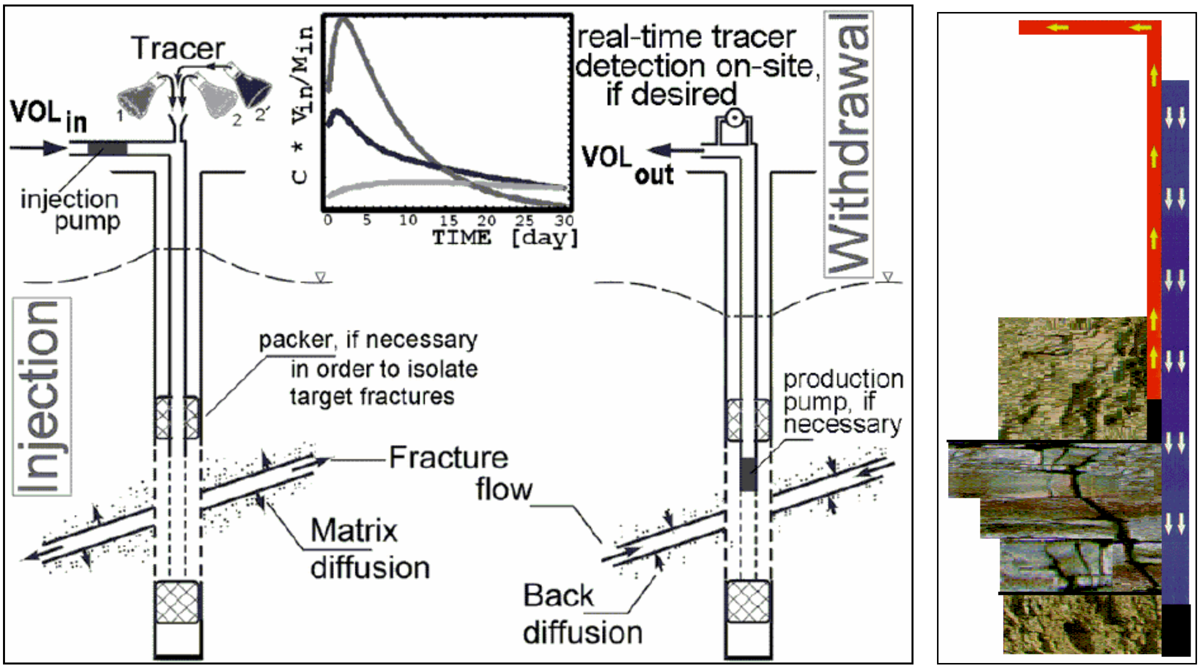

Figure 1c: Spiking application types (single-well injection-withdrawal, abbreviated as 'push-pull'; inter-well flow path tracing; single-well inter-horizon flow-path tracing).

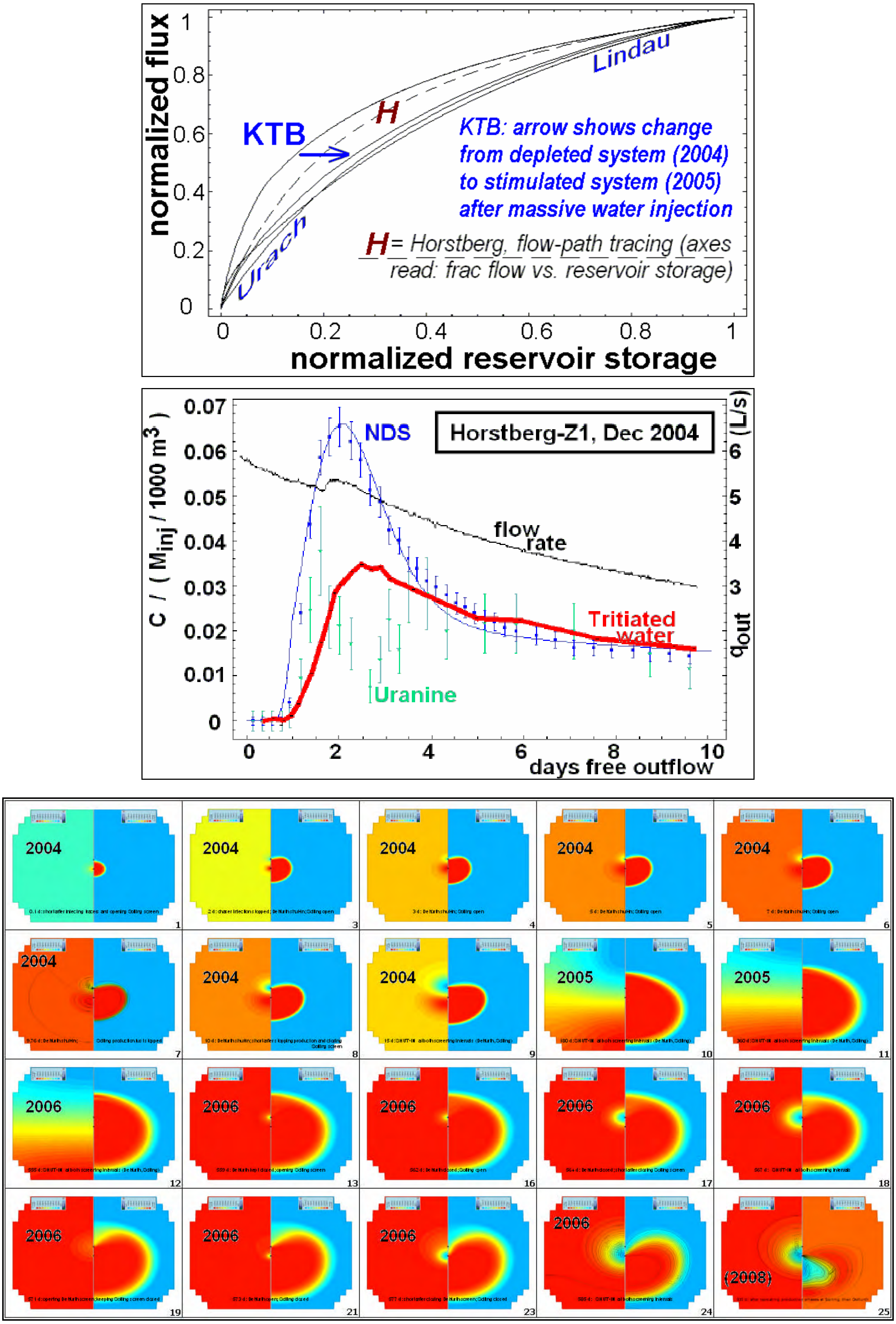

Figure 2: Flow-storage characteristics derived from various tests; SW tracing sequence (2004: FP tracing; 2006a: sampling for FP tracing continued; 2006b: SWIW-type withdrawal at lower horizon) in 4-km deep, supra-saline sedimentary formation at the Horstberg site.

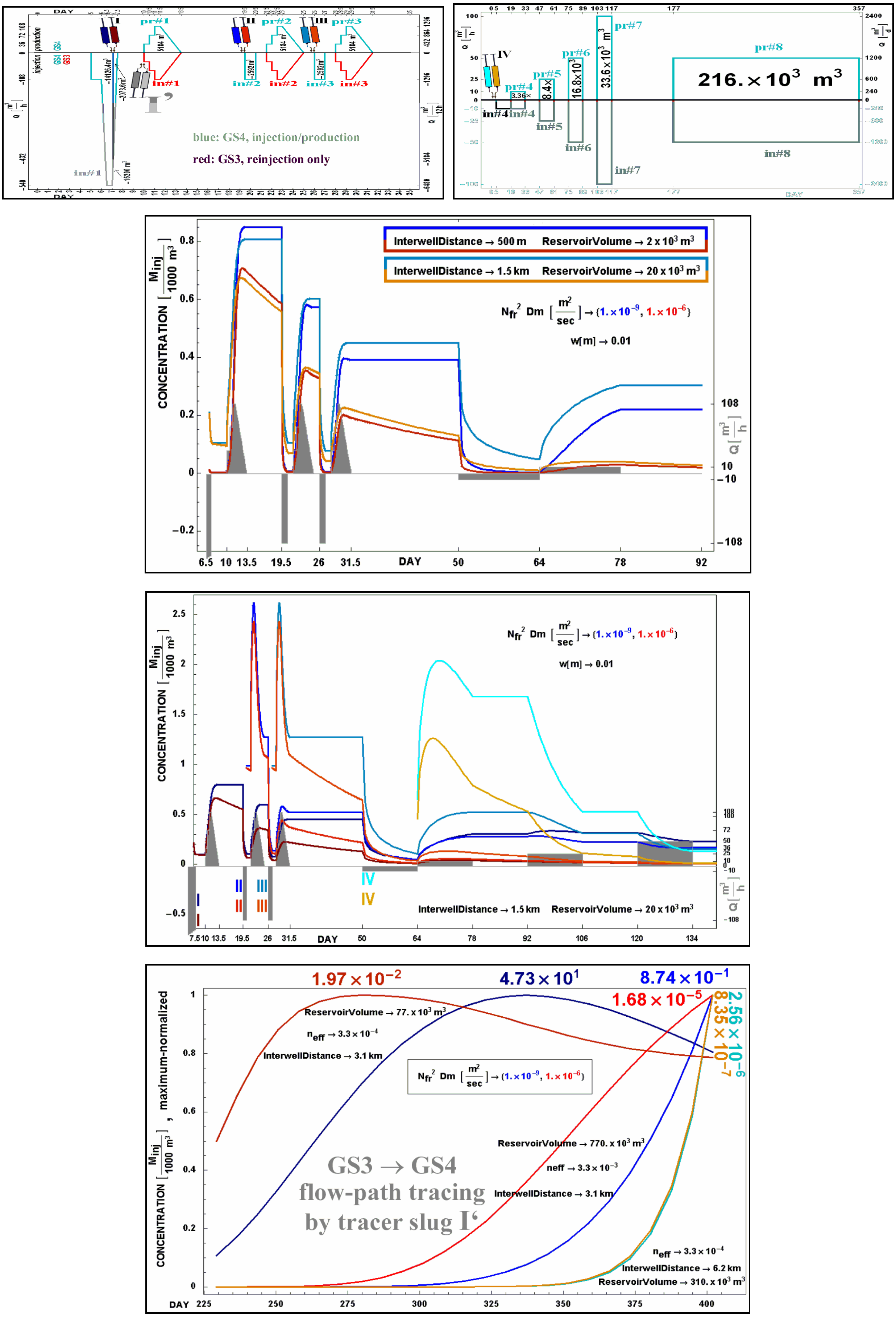

Figure 3: Single-well and inter-well spiking sequence (planned as of mid 2007) in 4-km deep, sub-saline sedimentary formations (sandstone, volcanics) at the GroßSchönebeck site.

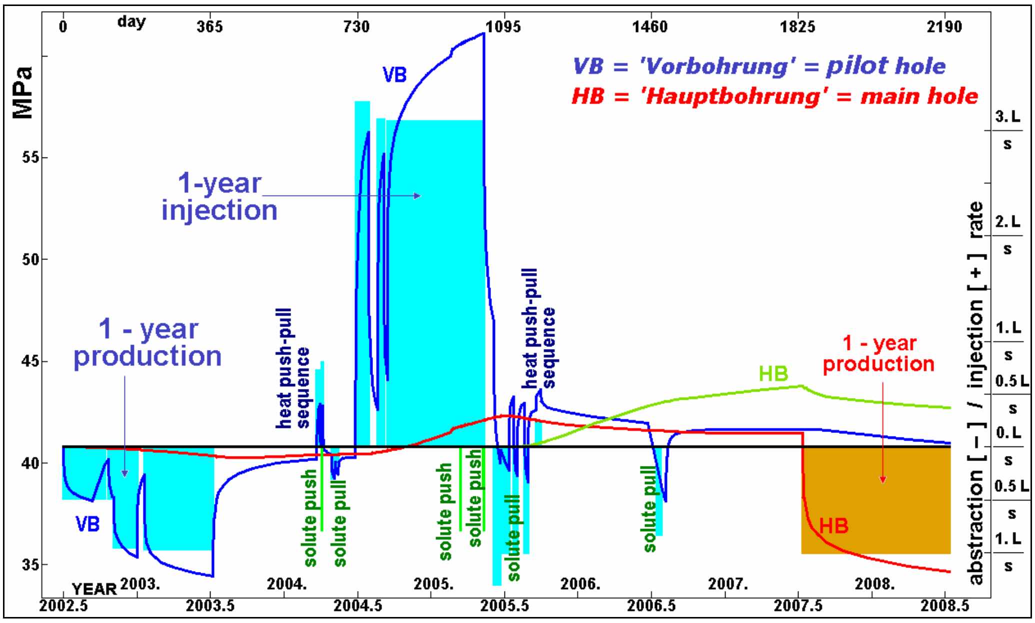

Figure 4: Sequence and concurrence of various hydraulic and tracer tests at the KTB site.

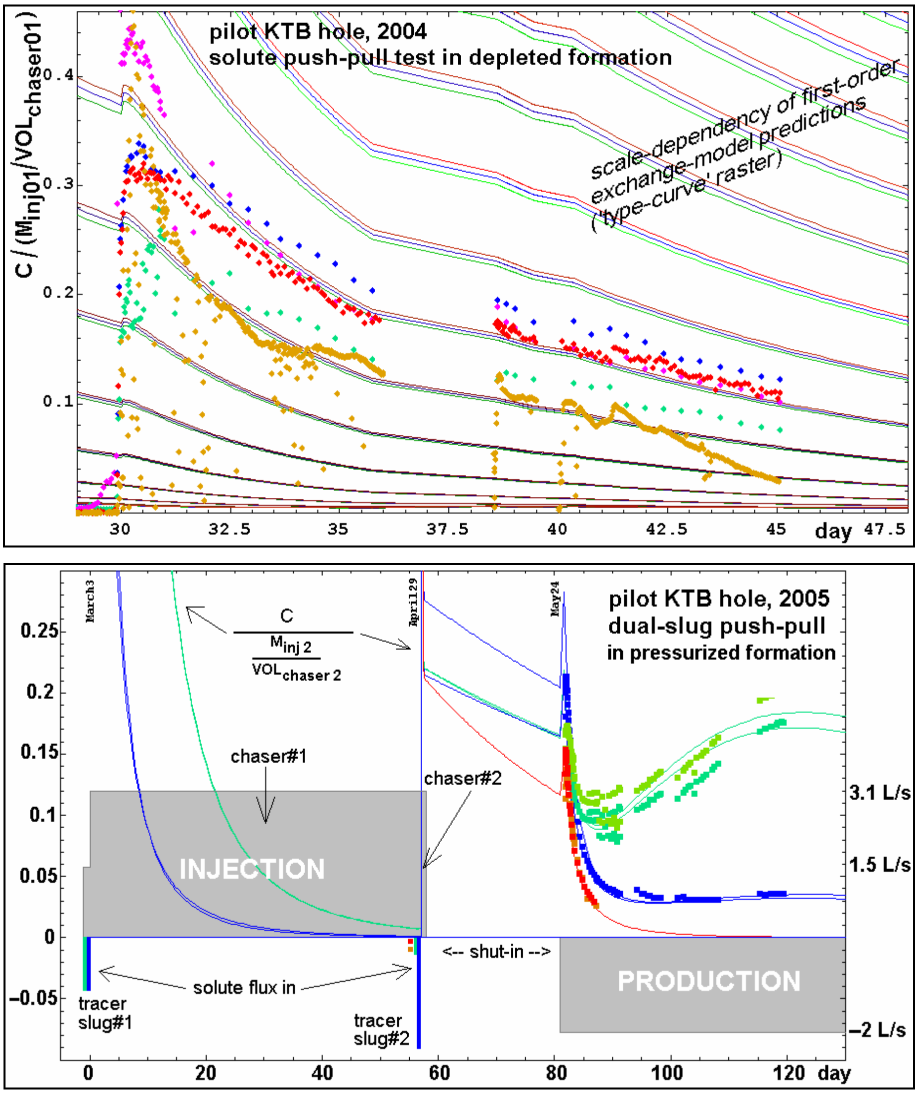

Figure 5: Solute tracer push-pull tests in depleted (2004) and stimulated (2005) state at the KTB site: measured tracer BTCs, and model fitting.

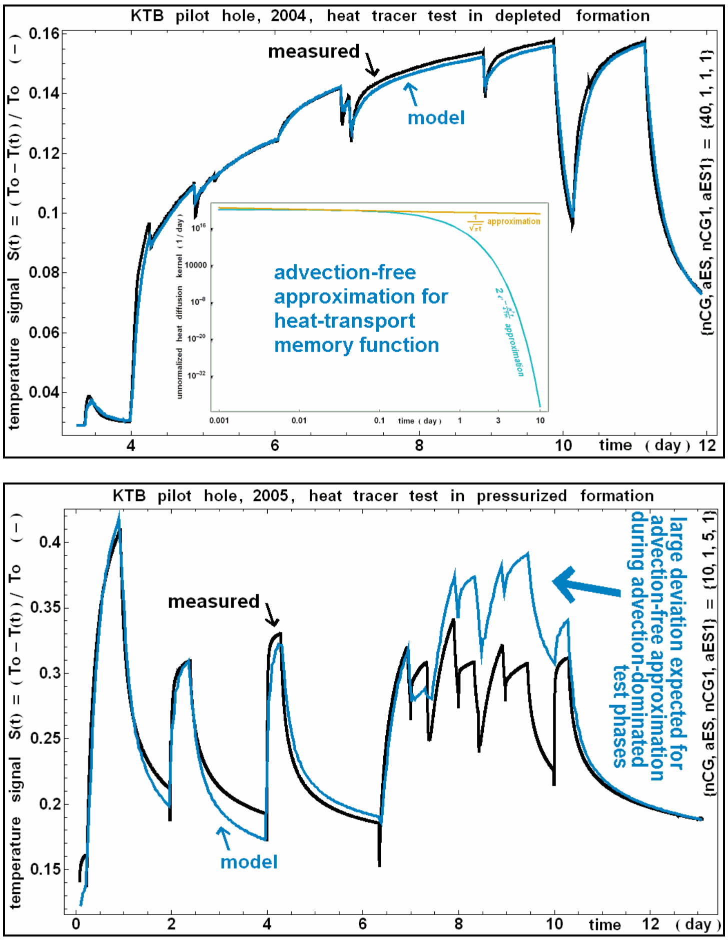

Figure 6: Heat push-pull sequences in depleted (2004) and stimulated (2005) state at the KTB site: in-situ temperature signal, and model fitting.

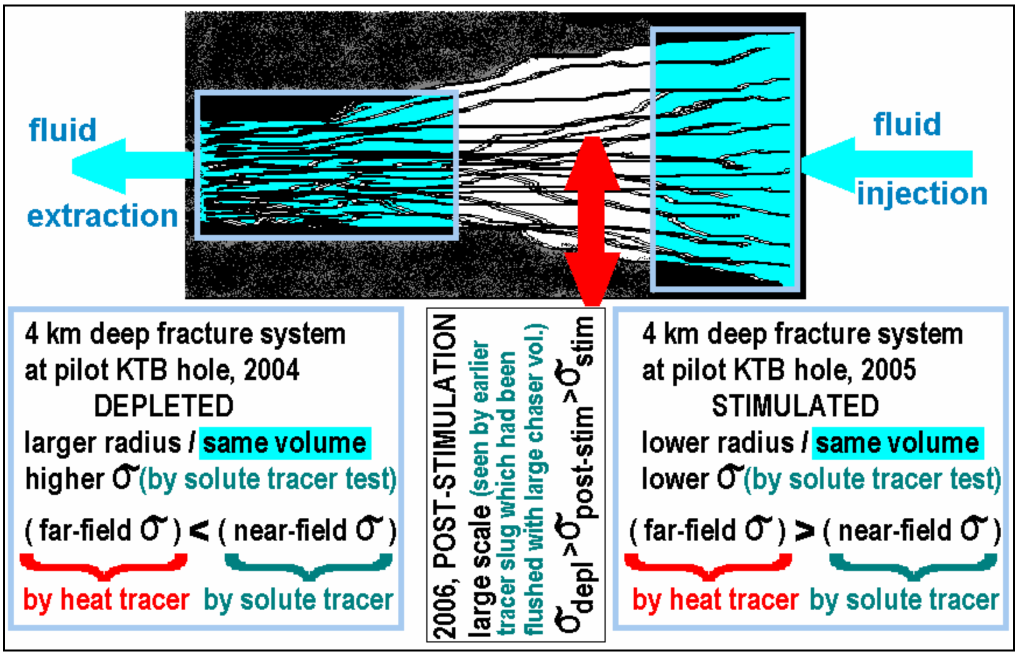

Figure 7: Interpretation of fracture network parameter changes during depletion and during stimulation. Shaded areas represent equal reference volumes; the same fluid volume corresponds to a larger radial extension in the depleted system, than in the stimulated system. During depletion, even some fractures that become hydraulically inactive may still contribute non-negligible tracer fluxes, thus indicating a higher fracture density. During stimulation, the prevailing process appears to be enlargement of pre-existing fractures, corresponding to a lowering of fracture density.

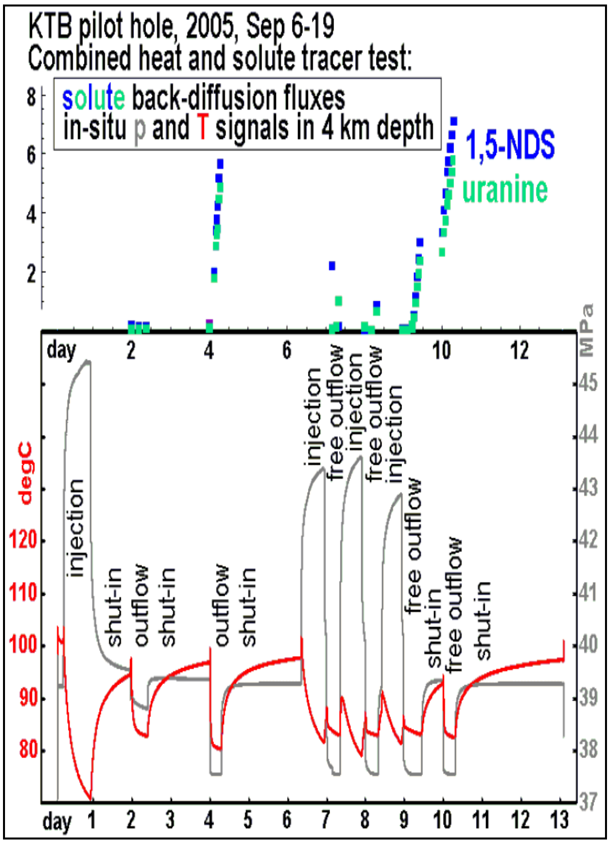

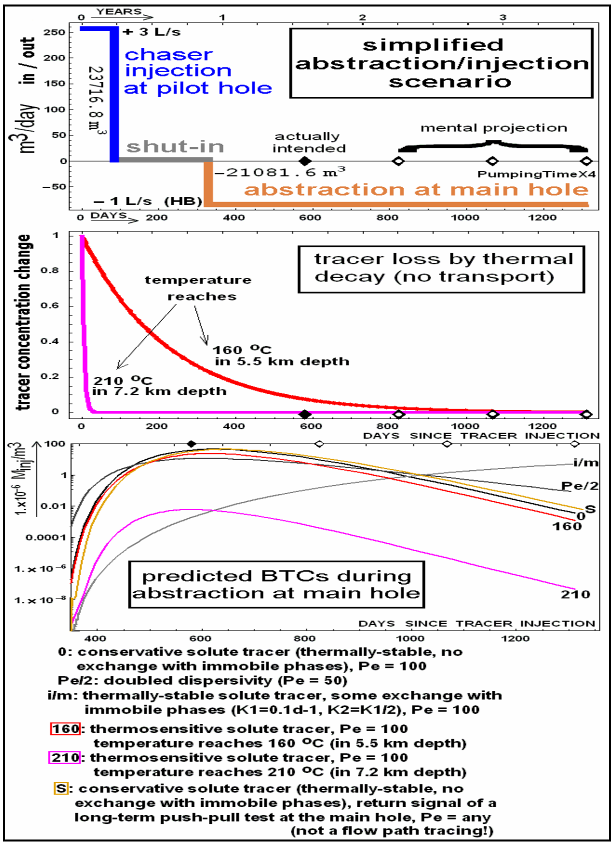

Figure 8: 'Dual' solute-tracer signals during short-term heat push-pull sequence in post-stimulation state at the KTB site.
Figure 9: Possible tracer BTCs at the main hole, against various transport and thermal decay scenarios.

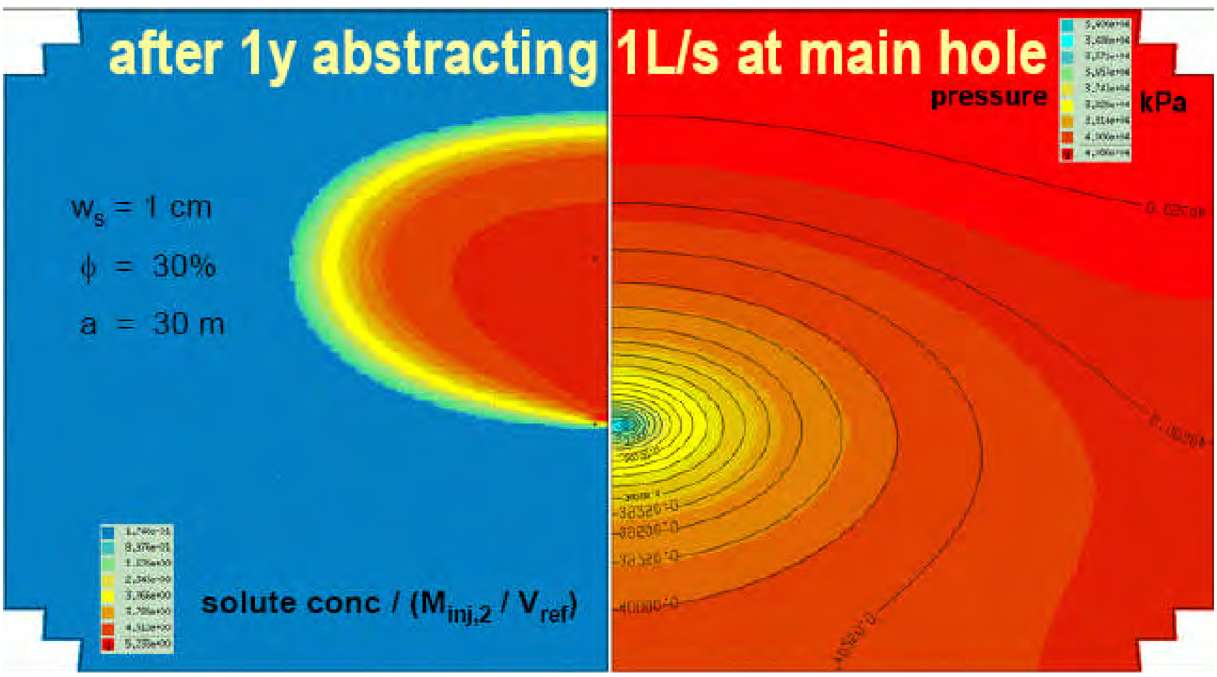

Figure 10: Simulated solute spreading between pilot hole and main hole at the KTB site, after assumed 1-year shut-in followed by 1 year abstracting 1L/s at the main hole; tracer dilution due to divergent spreading, and later on by large quantities of unspiked fluid.